Colloid Polym Sci (2004) 282: 486–494
DOI 10.1007/s00396-003-0972-4

ORIGINAL CONTRIBUTION

T. Okubo
S. Kanayama
K. Kimura

Dissipative structures formed in the course of drying the aqueous solution of *n*-dodecyltrimethylammonium chloride on a cover glass

Received: 24 March 2003
Accepted: 23 June 2003
Published online: 28 November 2003

T. Okubo (✉) · S. Kanayama · K. Kimura
Department of Applied Chemistry and Graduate School of Materials Science, Gifu University, Yanagido 1-1, 501-1193 Gifu, Japan
E-mail: okubotsu@apchem.gifu-u.ac.jp
Fax: +81-58-2932628

Abstract Macroscopic and microscopic dissipative structural patterns are formed in the course of drying an aqueous solution of *n*-dodecyltrimethylammonium chloride on a cover glass. Broad ring patterns of the hill accumulate with detergent molecules to form around the outside edges of the film solution in the macroscopic scale. The drying time (T) and the pattern area (S) decrease and increase respectively, as the detergent concentration increases. T decreases significantly as the ethanol fraction increases in the aqueous ethanol mixtures, whereas S increases as the fraction increases. Both T and S decrease as the concentrations of KCl, $CaCl_2$ or $LaCl_3$ increase. Cross-, branch-, and arc-like microscopic patterns are observed in the separated block regions. The convection of water and detergents at different rates under gravity and the translational and rotational Brownian movement of the latter are important for macroscopic pattern formation. Microscopic patterns are determined by the translational Brownian diffusion of the detergent molecules and the electrostatic and the hydrophobic interactions between the detergents and/or between the detergent and cell wall in the course of the solidification.

Keywords Drying dissipative structure · Pattern formation · Fractal pattern · *n*-Dodecyltrimethylammonium chloride

Introduction

It is well known that most patterns in nature and experiments in the laboratory form via self-organization accompanied with the dissipation of free energy and in the non-equilibrium state. Among several factors for free energy dissipation, evaporation and convection induced by the earth's gravity are very important for pattern formation.

Several papers on the pattern formation in the course of drying the monodispersed colloidal suspensions have been reported so far [1, 2, 3, 4, 5, 6, 7, 8, 9, 10, 11, 12, 13, 14, 15, 16]. Most of the papers have studied the liquid-like suspensions containing more or less ionic species. Electrostatic inter-particle interactions have been pointed out as an important factor in dissipative structures. Hydrophobic and hydrophilic interactions are also demonstrated to be important for the drying process [6, 14, 15]. Gelbart et al. [4, 5, 7] examined the mechanism of solvent dewetting in annular ring structures formed by drying a diluted metal colloid on a substrate. Shimomura et al. has studied intensively the dissipative patterns in the processes of film formation by drying polymer solutions [17].

In previous papers from our laboratory [18, 19], dissipative patterns on a cover glass have been observed in the course of drying colloidal crystal suspensions of colloidal silica and monodispersed polystyrene spheres, which are hydrophilic and hydrophobic in their surfaces, respectively. The colloidal crystal is undoubtedly one of the most simple and convenient systems for the study of

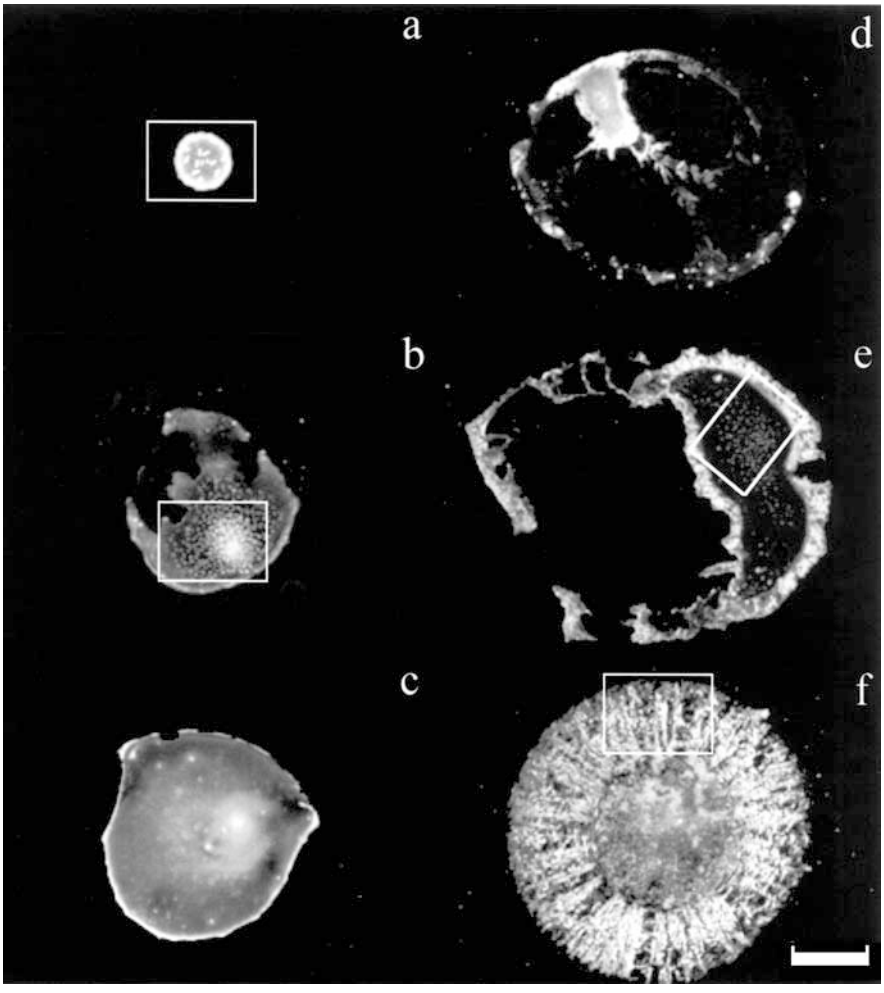

Fig. 1a–f Patterns formed for DTAC on a cover glass at 25 °C. **a** 1×10^{-6} M, **b** 1×10^{-5} M, **c** 2×10^{-5} M, **d** 1×10^{-4} M, **e** 1×10^{-3} M, **f** 1×10^{-2} M. In water, $V = 100$ μl, length of the bar is 1.0 mm

dissipative structures in the laboratory scale. For example, accurate structural information on the processes of dissipative pattern formation is available for colloidal crystal suspensions by use of reflection spectroscopy in real time.

Colloidal crystallization phenomena in a closed container, which are not dissipative structures but typical examples of the three-dimensional self-organization in the thermodynamically equilibrium state, have been studied intensively by many researchers including the authors' group [20, 21, 22, 23, 24, 25, 26, 27, 28, 29]. It has been clarified that the structural and kinetic properties of colloidal crystals are influenced strongly by electrostatic inter-particle repulsion via electrical double layers around the particles, the shape of colloidal particles, and the interaction between the particles and the cell wall of a sample container. For example, the densest crystal planes, 111 and 100 crystal planes for the face-centered-cubic (fcc) and body-centered-cubic (bcc) lattices, always orient parallel to the cell wall [30, 31]. Furthermore, colloidal crystallization rates are much higher for the plane cell than those for the tube cell [30].

Quite similar macroscopic and microscopic dissipative structural patterns formed between the colloidal silica and the polystyrene spheres. Spoke- and ring-like cracks formed in the macroscopic scale. The broad ring patterns of the hill accumulated with spheres formed around the outside edge. Fractal patterns of the sphere association were observed at the microscopic scale. Capillary forces between spheres at the air–liquid interface and the different rates of convection flows of water and solutes at the drying front were important for the macroscopic and microscopic pattern formation. Quite recently, the drying dissipative structures have been studied for the linear-type cationic polyelectrolyte, poly (allylamine hydrochloride) [32]. Macroscopic broad ring patterns, where the polymers accumulate densely in the outside edge, formed in many cases. Furthermore, beautiful fractal patterns were observed in the microscopic scale.

In this work, the experiments were made for *n*-dodecyltrimethylammonium chloride, which is one of the typical cationic detergent molecules. The main purpose of this work is to study what patterns are common

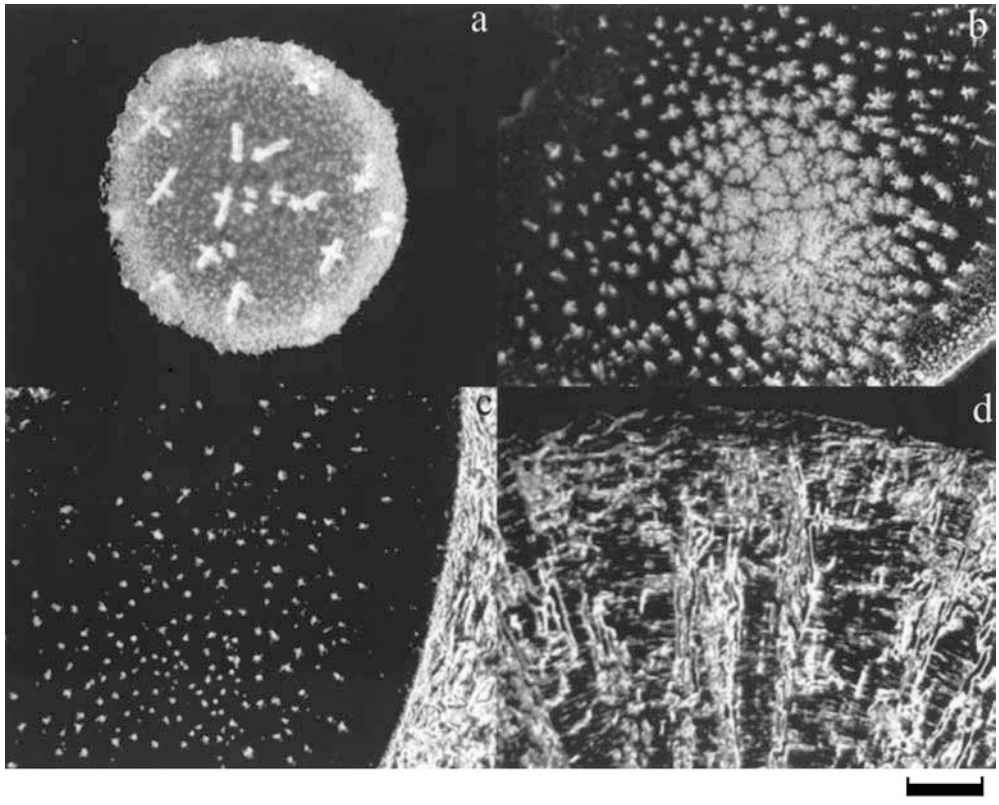

Fig. 2a–d Patterns formed for DTAC on a cover glass at 25 °C. **a** 1×10^{-6} M, **b** 1×10^{-5} M, **c** 1×10^{-3} M, **d** 1×10^{-2} M. In water, $V=100$ μl, length of the bar is 200 μm

and/or special among the many kind of solutes in solution and suspension states.

Experimental

Materials

n-Dodecyltrimethylammonium chloride (DTAC) for ion-pair chromatography was purchased from Tokyo Kasei Industries (Tokyo, Japan) and used without further purification. Potassium chloride (99.9%), calcium chloride dihydrate (99.9%) and lanthanum chloride heptahydrate (99.9%) were obtained from Wako Pure Chemical Industries (Tokyo, Japan). These simple electrolytes were also used without further purification. Ethanol (99.5%), used for rapid-scanning liquid chromatography, was also from Wako. Water used for the sample preparation was purified by a Milli-Q reagent grade system (Milli-RO5 plus and Milli-Q plus, Millipore, Bedford, Mass., USA).

Observation of the dissipative structures

50 μl or 100 μl of the aqueous solution of DTAC was dropped carefully and gently on a micro cover glass (30 mm×30 mm, thickness No. 1, 0.12–0.17 mm, Matsunami Glass Co., Kishiwada, Osaka, Japan) in a schale (60 mm in diameter, 15 mm in depth, Petri Co., Tokyo, Japan). The cover glass was used without further rinsing in most cases. The extrapolated value of the contact angle for pure water was $31\pm0.2°$ from the drop profile of a small amount of water (0.2, 0.4, 0.6, and 0.8 μl) on the cover glass. Part of the experiments was also made on a rinsed cover glass with a sulfuric acid solution of potassium dichromate. The extrapolated contact angle of the rinsed glass was $11\pm0.2°$. A pipette (1 ml, disposable serological pipette, Corning Laboratory Science Co., Corning, N.Y., USA) was used for the dropping. Macroscopic and microscopic observations were made for the film formed after the suspension was dried up completely on a cover glass in a room air-conditioned at 25°C and 65% in humidity of the air.

Macroscopic dissipative structures were observed with a digital HD microscope (type VH-7000, Keyence Co., Osaka, Japan). Microscopic structures were observed with a laser three-dimensional profile microscope (type VK-8500, Keyence) and a metallurgical microscope (Axiovert 25CA, Carl-Zeiss, Jena GmbH, Jena, Germany). Observation of the microscopic patterns was also made with an atomic force microscope (type SPA400, Seiko Instruments, Tokyo, Japan).

Results and discussion

Figure 1 shows the typical patterns formed in the drying the DTAC solutions at the concentrations ranging from 1×10^{-6} M to 0.01 M. At low concentrations, the pattern area shrank in the center and the broad ring regions distributed roundly in the outer edges. The ring patterns were observed at all the concentrations examined as is clear in the figure. At the highest concentration of 0.01 M a broad ring pattern occupied with a large amount of detergent molecules was observed at the outer

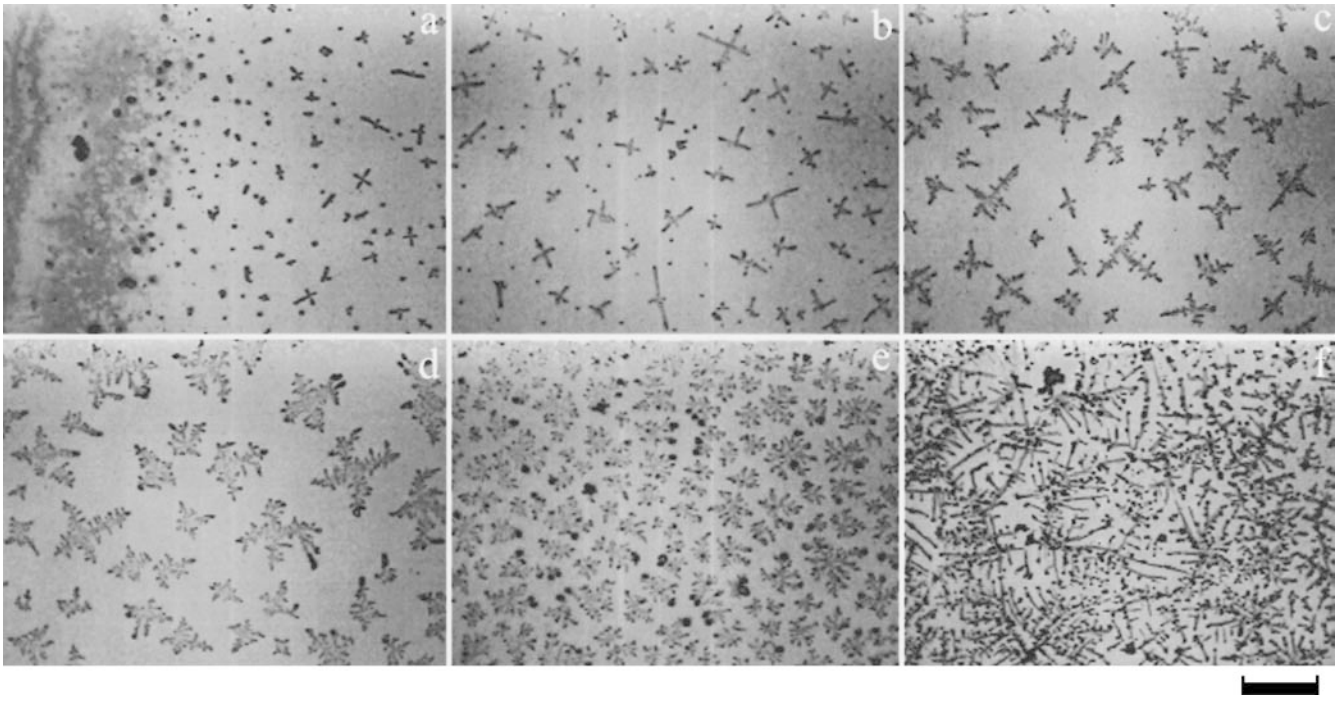

Fig. 3a–f Patterns formed for DTAC on a cover glass at 25°C. 2×10^{-5} M. In water, $V=100$ µl, **a**–**f** are places from the outside edge to the center, length of the bar is 20 µm

edge. It is mentioned here that macroscopic broad ring patterns were observed for most suspensions or solutions of colloidal silica [18], polystyrene spheres [19], India ink (Okubo et al., in preparation), and poly (allylamine hydrochloride) [32].

A main cause for the ring formation is undoubtedly due to the convection flow of the solvent and the detergent molecules. Most of the latter are in the form of associated micelles in solution. The flow of micelles from

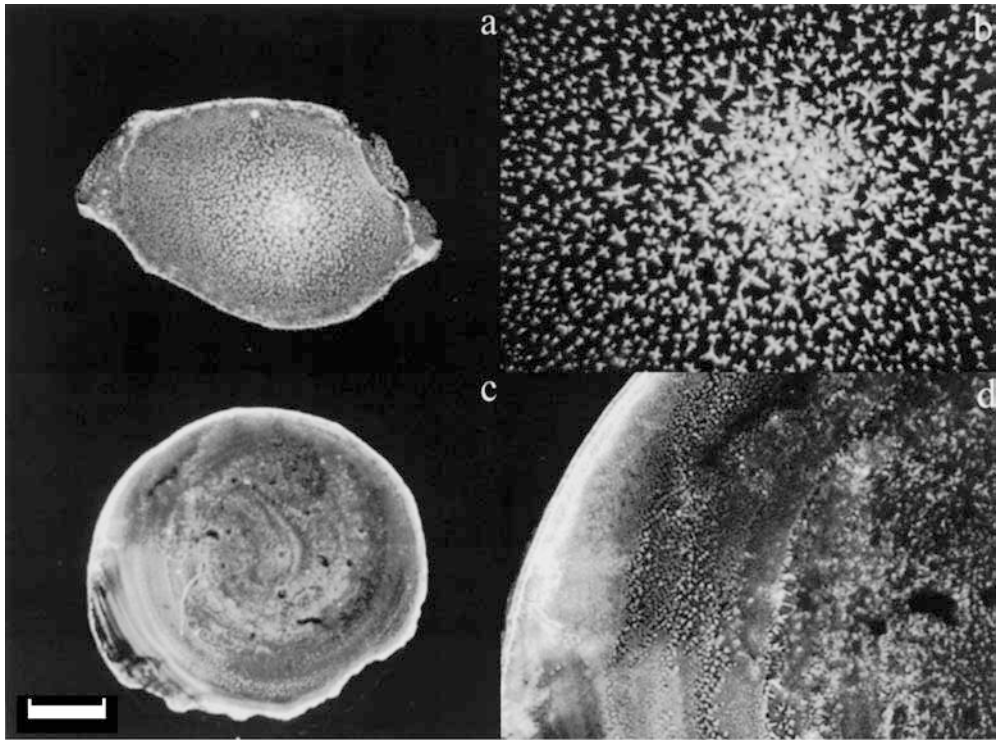

Fig. 4a–d Patterns formed for DTAC on a cover glass. **a** at 25 °C, length of the bar is 700 µm, **b** at 25 °C, 200 µm, **c** at 40 °C, 700 µm, **d** at 40 °C, 200 µm. 1×10^{-5} M, in water, $V=100$ µl

Table 1 T and S and the other parameters in the dissipative structures

[DTAC] (M)	Temp. (°C)	V (μL)	T (min)	S (mm_2)
1×10^{-7}	25	50	196	2.1
1×10^{-6}	25	50	205	7.0
1×10^{-5}	25	50	202	8.2
1×10^{-4}	25	50	199	10.7
1×10^{-3}	25	50	185	17.5
1×10^{-2}	25	50	160	25.3
1×10^{-7}	25	100	365 (1250)[a]	2.5 (1.2)[a]
1×10^{-6}	25	100	322 (1200)[a]	1.1 (2.1)[a]
1×10^{-5}	25	100	353 (1180)[a]	9.3 (10.3)[a]
1×10^{-4}	25	100	336 (1150)[a]	21.6 (7.2)[a]
1x10^{-3}	25	100	340 (1080)[a]	33.8 (7.2)[a]
1×10^{-2}	25	100	266 (1060)[a]	31.5 (20.3)[a]
1×10^{-7}	25	100	105[b]	_[b]
1×10^{-6}	25	100	111[b]	_[b]
1×10^{-5}	25	100	107[b]	_[b]
1×10^{-4}	25	100	255[b]	1.0[b]
1×10^{-3}	25	100	329[b]	13.6[b]
1×10^{-2}	25	100	301[b]	19.0[b]
1×10^{-6}	40	100	54	4.4
1×10^{-5}	40	100	70	16.1
1×10^{-4}	40	100	73	20.4
1×10^{-3}	40	100	69	24.0
1×10^{-2}	40	100	51	32.3
1×10^{-5}	25	100	267[c]	8.7[c]
1×10^{-2}	25	100	215[c]	29.5[c]
1×10^{-5}	25	100	212[d]	10.9[d]
1×10^{-2}	25	100	212[d]	30.0[d]
1×10^{-5}	25	100	173[e]	12.6[e]
1×10^{-2}	25	100	167[e]	27.6[e]
1×10^{-525}	100	130f	14.3[f]	
1×10^{-2}	25	100	116[f]	22.3[f]
1×10^{-6}	25	100	21[g]	—[g]
1×10^{-5}	25	100	29[g]	18.3[g]
1×10^{-4}	25	100	30[g]	16.2[g]
1×10^{-3}	25	100	34[g]	15.7[g]
1×10^{-2}	25	100	25[g]	19.3[g]
1×10^{-5}	25	100	382[h]	18.2[h]
1×10^{-5}	25	100	395[i]	18.1[i]
1×10^{-5}	25	100	360[j]	11.4[j]
1×10^{-5}	25	100	395[k]	17.6[k]
1×10^{-5}	25	100	390[l]	19.9[l]
1×10^{-5}	25	100	377[m]	11.5[m]
1×10^{-5}	25	100	388[n]	16.2[n]
1×10^{-5}	25	100	333[o]	14.5[o]
1×10^{-5}	25	100	290[p]	11.0[p]

[a]The data in parentheses are for the condition with covering the sample shale.
[b]The data of T and S are observed for the rinsed cover glass.
[c]Ethanol 20%.
[d]Ethanol 40%.
[e]Ethanol 60%.
[f]Ethanol 80%.
[g]Ethanol 100%.
[h]KCl, 1×10^{-6}M.
[i]KCl, 1×10^{-5}M.
[j]KCl, 1×10^{-4}M.
[k]$CaCl_2$, 1×10^{-6}M.
[l]$CaCl_2$, 1×10^{-5}M.
[m]$CaCl_2$, 1×10^{-4}M.
[n]$LaCl_3$, 1×10^{-6}M.
[o]$LaCl_3$, 1×10^{-5}M.
[p]$LaCl_3$, 1×10^{-4}M.

the center area toward the outside edges is especially enhanced by the evaporation of water at the liquid surface of the outside edges, resulting in the lowering of the solution temperature in the upper region of the liquid area. When the micelles reach the edges of the drying frontier at the outside region of the liquid, part of the micelles go back to the center. However, the movement of most of the micelles stops owing to the solidification (crystallization) at the frontier region by the disappearance of water. This process must be followed by the broad ring-like accumulation of the detergent molecules near the round edges. It should be noted here that the importance of the convection flow of colloidal spheres and polymers for ring formation was also proposed by other researchers in the process of the film formation [9, 33].

Figure 2 shows the close-up detail of the square areas shown in Fig. 1a, b, e, f. The length of the bar is 200 μm. The patterns of Fig. 2a, b, and c are composed of sharp crosses, which must be formed in the solidification above the solubility of DTAC in the drying process. The detergent concentration should distribute roundly in the course of drying by the dissipative convection flow. Thus, shape and size differ delicately as a function of the distance from the center. At the concentration 1×10^{-5} M in Fig. 2b, beautiful fractal patterns composed of crosses were observed in the separated block regions. Of course, these patterns form in a semi-equilibrium state above the solubility in the gradient detergent concentration distribution by the dissipative convection flow. It should be mentioned here that the patterns shown in Fig. 2b are quite similar to those for aqueous solution of poly (allylamine hydrochloride) shown in Fig. 2c of ref. [32]. Although these two molecules are the same in the sense of cationic solutes, they differ in size, shape, and flexibility of their conformation.

Patterns in the broad ring region shown in Fig. 2d at a high concentration of DTAC (0.01 M) are composed of fine rings and spokes, which are crossed or netted to each other. The kinetic study of the pattern formation in the course of drying is interesting and its study is now in progress in our laboratory, using a time-resolved digital CCD camera.

Figure 3 shows close-up detail at 2×10^{-5} M. Fig. 3a–f are the extended patterns observed from the edge region to the center. Clearly, the patterns are cross-like irrespective of the location. However, the patterns become large and complex and the blocks are separated. In the center region, curved long lines are also observed as is shown in Fig. 3f.

Figure 4a and b show the macroscopic and microscopic patterns observed in the condition of the covered schale, but at the same concentration and temperature (1×10^{-5} M at 25°C) as shown in Fig. 1b and Fig. 2b. Surprisingly, the patterns with and without cover are quite similar to each other, though the T and S values increase substantially and decrease by

covering the solution as is clear in Table 1. Figure 4c and d show the observations at 40 °C without cover. When the drying temperature is high, both T and S decreased. Furthermore, the dissipative patterns at 40 °C differ significantly from those at 25 °C, and are similar to the surface pattern of a Japanese earthenware called "Shigaraki Yaki". These observations support strongly that the drying patterns are determined mainly by the relative rates of the convection flow of the solutes and the solvent. At low temperature, the patterns will form after achieving the stable convection flow of solutes. At high temperature, however, the drying rate of the solvent is so high that the patterns will form in the middle of the solute convection process. It should be noted here that the microscopic fractal patterns were observed in the rather narrow range of detergent concentrations from 10^{-5} M to 10^{-4} M. No fractal patterns were observed for the more diluted and also more concentrated detergent solutions. This feature is also quite similar to the cationic polyelectrolytes [32].

Figure 5 shows the expanded patterns observed for the aqueous ethanol solutions. The patterns were composed of small blocks ca. 10 mm in size and quite similar to those observed for the dried pattern at high temperature (see Fig. 4d). Selective evaporation of ethanol component takes place for the aqueous ethanol mixtures resulting in rapid convection flow, since the boiling point of ethanol (78 °C at 1 atm) is low compared with that of water (100 °C).

The microscopic patterns of DTAC molecules coexisting with KCl, $CaCl_2$ and $LaCl_3$ are shown in Figs. 6, 7 and 8, respectively. When the concentrations of the detergent and salt are comparable to each other (see Figs. 6b, c, 7c, 8b and c), tree branch and arc-like patterns were observed, which are entirely different from those of the purely detergent or salt solutions. The patterns are also similar to the microscopic structures of poly (allylamine hydrochloride) (see Fig. 3 of ref. [32], for example). These results suggest that the micelle structure of DTAC molecules is in the form of a long rod in the solution just before the solidification.

Concluding remarks

Macroscopic broad ring patterns were observed for all the solutes examined, i.e., colloidal spheres [1, 2], cationic polymer [32], and detergent molecules in this work. A part of the microscopic patterns was quite similar to those of the polymer. It should be recalled here that for the colloidal spheres, the nature of the solutes was not so essential for the formation of the dissipative structures. Furthermore, size of spheres was not so important for the pattern formation, but instead the spherical shape itself was essential. For the polymer and DTAC

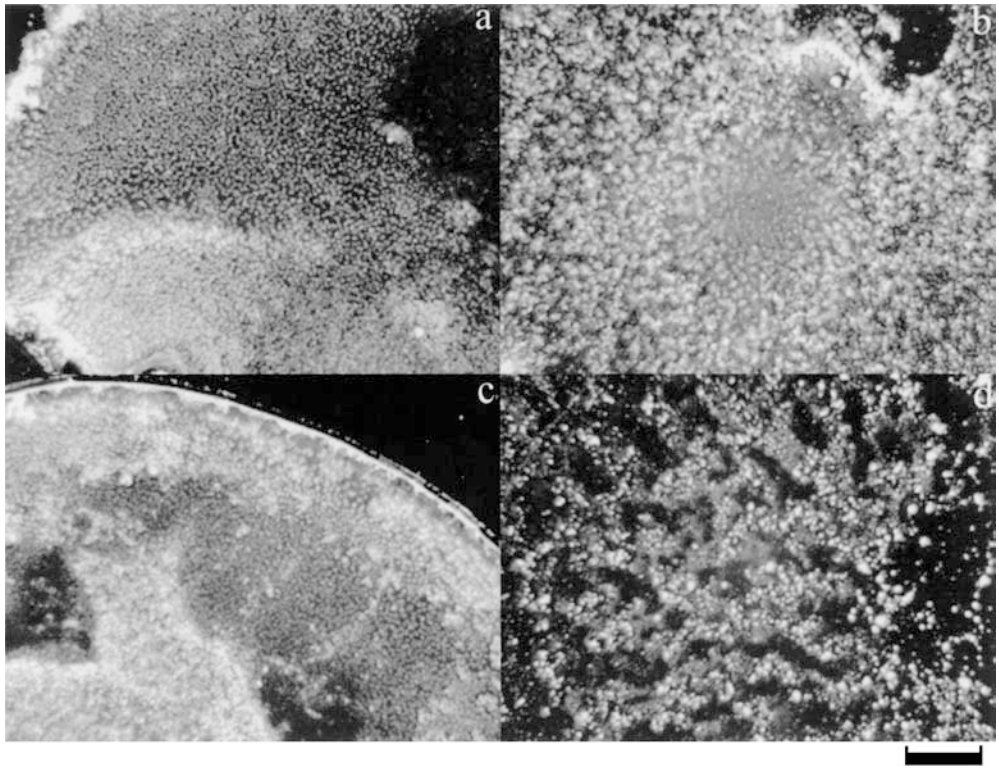

Fig. 5a–d Patterns formed for DTAC in aqueous ethanol solution on a cover glass at 25 °C. **a** Ethanol content: 20%, **b** 40%, **c** 80%, **d** 99.5%, 1×10^{-5} M, in water, $V=100$ μl, length of the bar is 200 μm

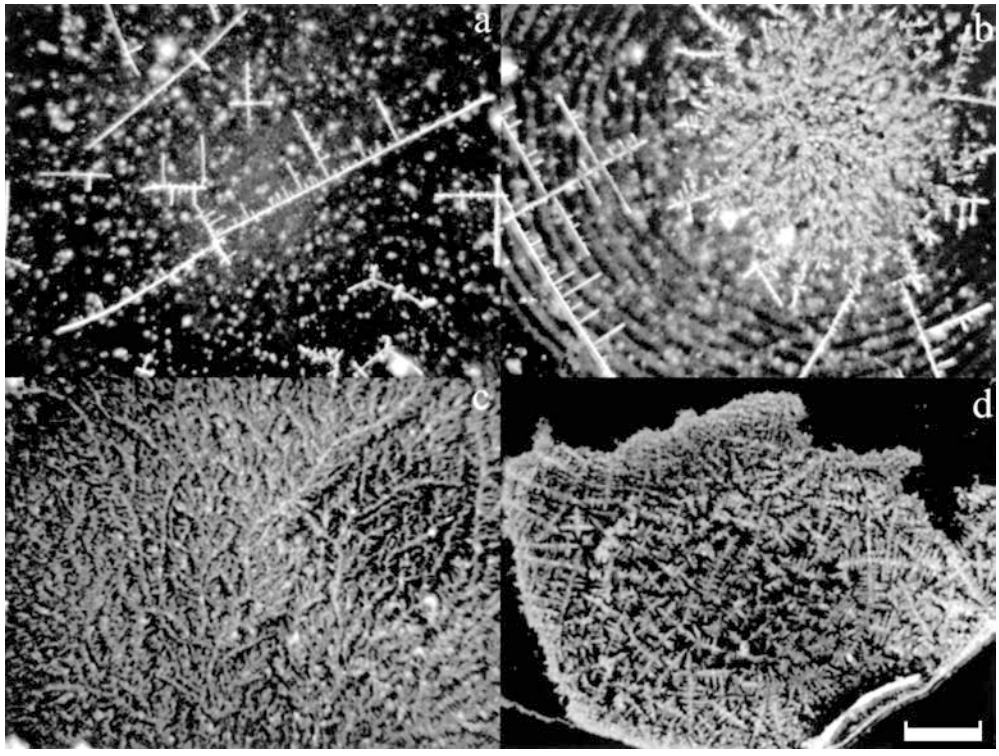

Fig. 6a–d Patterns formed for DTAC on a cover glass at 25 °C. **a** [DTAC] = 2×10^{-5} M, [KCl] = 1×10^{-6} M, **b** 2×10^{-6} M, 1×10^{-5} M, **c** 2×10^{-5} M, 1×10^{-4} M, **d** 0 M, 1×10^{-5} M, in water, $V = 100$ µl, length of the bar is 200 µm

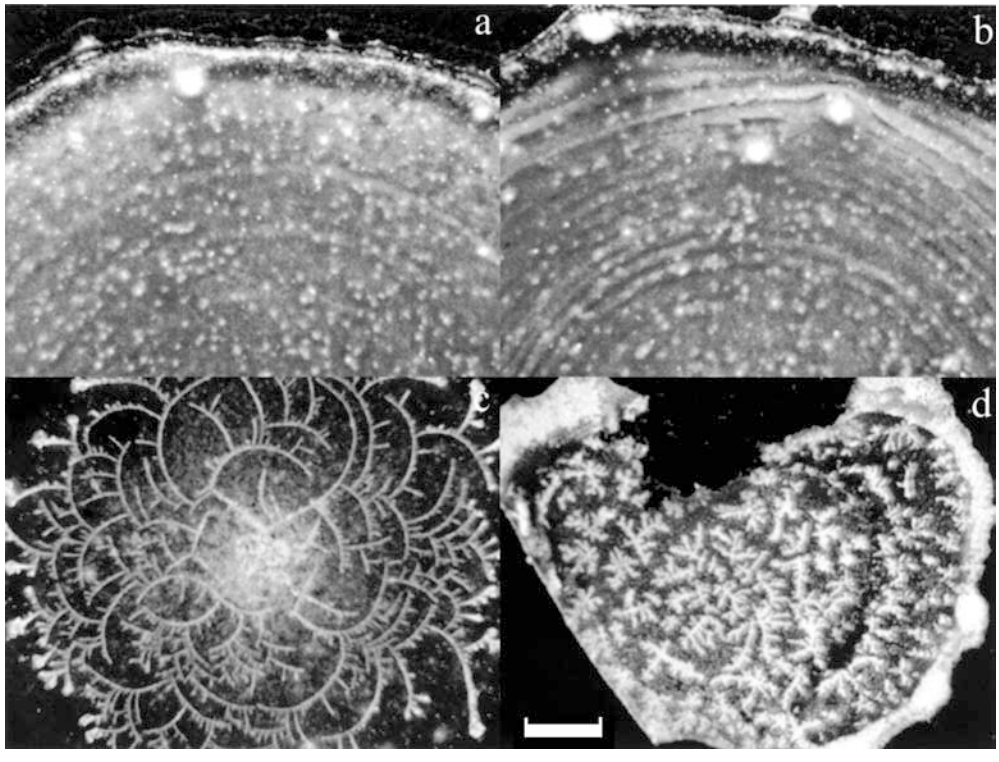

Fig. 7a–d Patterns formed for DTAC on a cover glass at 25 °C. **a** [DTAC] = 2×10^{-5} M, [$CaCl_2$] = 1×10^{-6} M, **b** 2×10^{-6} M, 1×10^{-5} M, **c** 2×10^{-5} M, 1×10^{-4} M, **d** 0 M, 1×10^{-5} M, in water, $V = 100$ µl, length of the bar is 200 µm

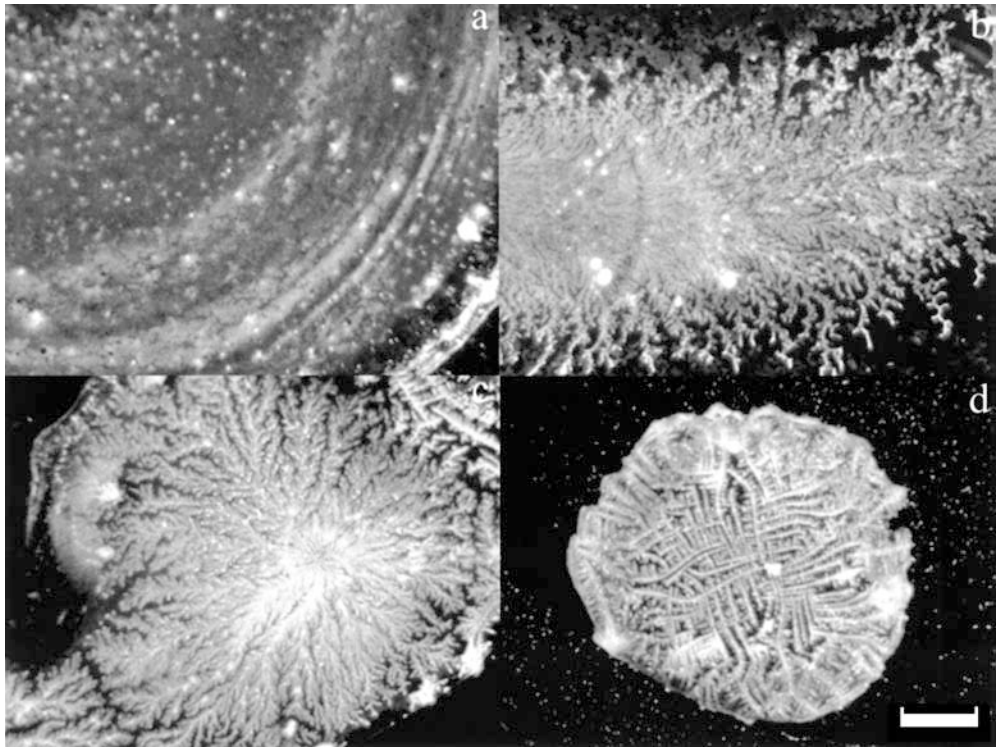

Fig. 8a–d Patterns formed for DTAC on a cover glass at 25 °C. **a** [DTAC] = 2×10^{-5} M, [$LaCl_3$] = 1×10^{-6} M, **b** 2×10^{-6} M, 1×10^{-5} M, **c** 2×10^{-5} M, 1×10^{-4} M, **d** 0 M, 1×10^{-5} M, in water, $V = 100$ μl, length of the bar is 200 μm

solution, however, the specific association between the solutes in the course of dryness plays an important role for the microscopic pattern formation. In other words, microscopic patterns may differ greatly depending on the kind and nature of the solutes. It should be noted that the microscopic patterns are determined by the translational Brownian diffusion of the detergent molecules and the electrostatic and the hydrophobic interactions between the detergents and/or between the detergent and the cell wall in the course of the solidification.

Acknowledgements The Ministry of Education, Science, Sports and Culture is thanked for grants-in-aid for Scientific Research on Priority Area (A) (11167241) and for Scientific Research (B) (11450367).

References

1. Vanderhoff JW (1973) J Polymer Sci Symp 41:155
2. Nicolis G, Prigogine I (1977) Self-organization in non-equilibrium systems. Wiley, New York
3. Cross MC, Hohenberg (1993) Rev Mod Phys 65:851
4. Ohara PC, Heath JR, Gelbart WM (1997) Angew Chem 109:1120
5. Ohara PC, Heath JR, Gelbart WM (1998) Langmuir 14:3418
6. Uno K, Hayashi K, Hayashi T, Ito K, Kitano H (1998) Colloid Polymer Sci 276:810
7. Gelbart WM, Sear RP, Heath JR, Chang S (1999) Faraday Discuss 112:299
8. Van Duffel B, Schoonheydt RA, Grim CPM, De Schryver FC (1999) Langmuir 15:7520
9. Maenosono S, Dushkin CD, Saita S, Yamaguchi Y (1999) Langmuir 15:957
10. Brock SL, Sanabria M, Suib SL, Urban V, Thiyagarajan P, Potter DI (1999) J Phys Chem 103:7416
11. Nikoobakht B, Wang ZL, El-Sayed MA (2000) J Phys Chem 104:8635
12. Ge G, Brus L (2000) J Phys Chem 104:9573
13. Chen KM, Jiang X, LC Kimerling, Hammond PT (2000) Langmuir 16:7825
14. Lin XM, Jaenger HM, Sorensen CM, Klabunde (2001) J Phys Chem 105:3353
15. Kokkoli E, Zukoski CF (2001) Langmuir 17:369
16. Ung T, Liz-Marzan, Mulvaney (2001) J Phys Chem B 105:3441
17. Shimomura M, Sawadaishi T (2001) Curr Opin Colloid Interface Sci 6:11
18. Okubo T, Okuda S, Kimura H (2002) Colloid Polymer Sci 280:454
19. Okubo T, Kimura K, Kimura H (2002) Colloid Polymer Sci 280:1001
20. Vanderhoff W, van de Hul HJ, Tausk RJM, Overbeek JThG (1970) In: Goldfinger G (ed) Clean surfaces: their preparation and characterization for interfacial studies. Dekker, New York
21. Hiltner PA, Papir YS, Krieger IM (1971) J Phys Chem 75:1881

22. Kose A, Ozaki M, Takano K, Kobayashi Y, Hachisu S (1973) J Colloid Interface Sci 44:330
23. Mitaku S, Ohtsuki T, Kishimoto A, Okano K (1980) Biophys Chem 11:411
24. Lindsay HM, Chaikin PM (1982) J Chem Phys 76:3774
25. Pieranski P (1983) Contemp Phys 24:25
26. Ottewill RH (1985) Ber Bunsenges Phys Chem 89:517
27. Aastuen DJW, Clark NA, Cotter LK, Ackerson BJ (1986) Phys Rev Lett 57:1733
28. Pusey PN, van Megen W (1986) Nature 320:340
29. Okubo T (1988) Acc Chem Res 21:281
30. Okubo T (1997) Curr Topics Colloid Interface Sci 1:169
31. Okubo T (2002) In: Hubbard A (ed) Encyclopedia of surface and colloid science. Dekker, New York, p 1300.
32. Okubo T, Kanayama S, Ogawa H, Hibino M, Kimura K (2003) Colloid Polymer Sci (in press).
33. Latterini L, Blossey R, Hofkens J, Vanoppen P (1999) Langmuir 15:3582